Arezoo Ghanbari*, Masoud Alizadeh, Ebrahim Ghasemi, Rahim Yazdani Rad and Somaye Ghaffari

Preparation of optimal feedstock for low-pressure injection molding of Al/SiC nanocomposite

Abstract: This study aims to prepare optimal feedstock for fabrication of Al/SiC nanocomposites by the low-pressure injection molding technique. For this purpose, micron-sized aluminum and nanosized SiC powders were mixed with different amounts of the binder consisting of 89 wt% paraffin wax, 9 wt% bees wax, and 2 wt% stearic acid. Rheometry analyses as well as the Weir model were utilized to determine the optimal feedstock with the desired rheological properties and high homogeneity. Considering powder to binder ratios, shear sensitivity, flow activation energy, and homogeneity within the rheometry analyses, the feedstock of 78 wt% powder loading is selected as the optimal sample for injection molding. Investigation of optimal feedstock by the scanning electron microscopy technique also verified the high homogeneity of this feedstock. In addition, it was observed that all of the feedstocks had thixotrop behavior.

Keywords: Al/SiC; injection molding; moldability index; nanocomposites; rheology.

***Corresponding author: Arezoo Ghanbari,** Materials and Energy Research Center, P.O. Box 14155-4777, Tehran, Iran, e-mail: ar-ghanbari@merc.ac.ir
Masoud Alizadeh, Rahim Yazdani Rad and Somaye Ghaffari: Materials and Energy Research Center, P.O. Box 14155-4777, Tehran, Iran
Ebrahim Ghasemi: Institute for Color Science and Technology, P.O. Box 16765-654, Tehran, I ran

1 Introduction

Aluminum and its alloys have been extensively used for fabricating metal matrix composites (MMCs) due to their low density, high strength, and good corrosion resistance [1]. They are of highly preferred in vehicle weight reduction due to their availability as lightweight structural materials. Application of lightweight structural materials results in the reduction of fuel consumption and air pollution caused by vehicle emissions. The main problem which limits the application of light metals in engineering applications is their poor mechanical properties such as low elastic modulus, insufficient wear resistance, and high thermal expansion coefficient. Mechanical and thermal properties of aluminum-based alloys such as the aforementioned ones can be enhanced by preparing Al composites with ceramic materials such as SiC compound [2].

The physical and chemical compatibility between the aluminum matrix and the SiC particle is the main concern in preparing Al/SiC composites. Among the various reinforced MMCs, the Al/SiC systems, e.g., aluminum alloys reinforced either by SiC whiskers or SiC particles, are the most widely investigated and utilized ones due to their promising properties [2]. The addition of SiC particles leads to an increase in the wear resistance and elastic modulus as well as improvement of the thermal expansion coefficient [3, 4]. Furthermore, aluminum silicon carbide (Al/SiC) composites have desired thermal management performance which makes them suitable for microelectronics applications [5].

Metal injection molding is a promising method for the fabrication of various MMCs. The major advantages of this technology in comparison with the traditional powder metallurgy methods are high product density, more intricate shape, higher mechanical properties, and better surface finish [6]. Injection molding basically includes four steps: mixing, molding, debinding, and sintering [7, 8].

The molding stage, which determines the shape of the green body, plays an important role in the injection molding process. To fabricate specimens free of defects such as cracks and distortion, the study of rheological behavior of feedstock is of foremost concern [9–12].

The powder to binder ratio (termed as powder loading) of the mixing process is the main parameter that determines the success or failure of the subsequent steps of powder injection molding (PIM). A suitable feedstock for PIM is the one as concentrated as possible (more powder, less binder) in order to reduce the slump and shrinkage during debinding and sintering. On the one hand, insufficient binder can cause inappropriate molding and voids formation throughout. On the other hand, excessive binder reduces the feedstock viscosity which can result in powder-binder separation during molding. In fact, feedstock and the powder should be a homogenous mixture which is completely dispersed in the binder to obtain uniform and isotropic shrinkage during debinding and sintering [13, 14]. There is a critical powder loading at which the binder is just sufficient to completely fill the interparticulate voids. Critical powder loading in injection molding is a function of particles' size and shape, and composition and properties of binder [15]. For preparation of smooth surfaces and uniform structures by means of PIM, nanopowders should be applied. In this regard, fine powders of SiC and Al have the capability to preserve the smooth surface of Al/SiC composites prepared by the PIM method. This study is conducted to find the critical powder loading for preparation of Al/SiC nanocomposites.

Rheology is an important and elaborate method to study properties of liquids, suspensions, pastes, slurries, and semisolid materials. This technique has been frequently utilized in various ceramic processing techniques such as slip casting and injection molding for the study of slurries and semisolid pastes. With the application of rheometry, one can cost-effectively examine the homogeneities, viscosity, and fluid characteristics of injection molding feedstock [6, 7, 16, 17]. In this study, critical powder loading for preparation of Al/SiC nanocomposites by low-pressure injection molding has been determined by application of rheometry analysis as well as the scanning electron microscopy (SEM) technique.

2 Materials and methods

2.1 Materials

Al and SiC powders were purchased from (Khorasan Powder Metallurgy, Iran) and (MKnano, Canada) companies and applied as metal and reinforcement powders, respectively. Prior to PIM, the starting materials were examined by densitometry, electron microscopy, and dynamic light scattering methods in order to determine their primary density, particle shape, and particle size distribution. Results of this analysis showed that the aluminum and silicon carbide powders have pycnometer density of 2.7 g/cm^3 and 3.07 g/cm^3, respectively, while the corresponding primary particle sizes are d50=28 µm and d50=40 nm, respectively. The morphologies of the powders are also depicted in Figure 1. The particle shapes of the powders were studied by means of Philips CM-200 FEG transmission electron microscopy (TEM) and S-4160 Hitachi SEM. Al powders were of micron sizes (average 10 µm) with spherical shape, while the SiC nanopowders were less spherical and of particle size ranging from 40 to 100 nm. A Fritch analystte 22 Particle size analyzer was utilized to measure the particle size distributions of the powders. The densities of the powders were determined by an AccuPyc 1330 helium pycnometer.

In this study, the wax-based binder was selected for PIM due to its facile debinding capability. The binder composition and the characteristics of its components are listed in Table 1.

2.2 Procedure

Aluminum powder (95 wt%) and silicon carbide powder (5 wt%) were mixed by a planetary ball mill. Stearic acid (2 wt%) was also added to the powders as a lubricant to avoid agglomeration of the powders during the milling. The ball-milling experiment was performed in a high-energy planetary ball mill at a rotation speed of 250 rpm in argon atmosphere with ball-to-powder ratio of 10:1 for 1 h using the chrome steel balls. The mixed powders were

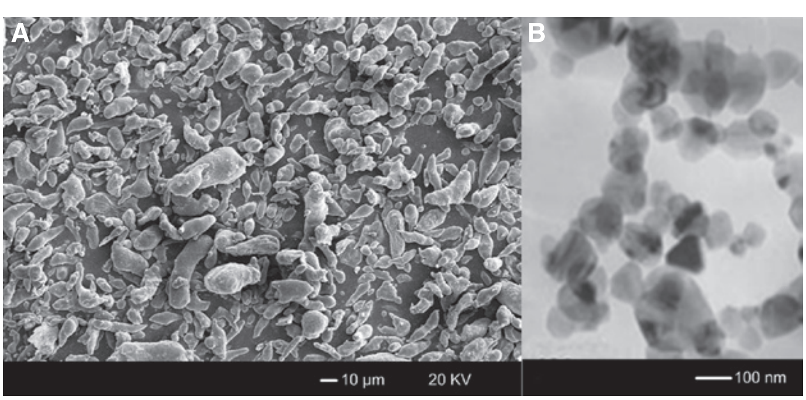

Figure 1 (A) SEM image of original Al micro-powders, (B) TEM image of SiC nanoparticles.

Table 1 The characteristics of the binder components.

Binder components	Components value	Chemical structure	Melting point (°C)	Decomposition temperature (°C)	Table density (g/cm³)
Paraffin wax	89	$C_{20}H_{42}$	75	200–400	0.90
Bees wax	9	$C_{15}H_{31}COOC_{30}H_{61}$	66	200–400	0.96
Stearic acid	2	$CH_3(CH_2)_{16}COOH$	63	383	0.96

Table 2 The characteristics of the feedstocks.

Feedstock	A	B	C	D
Powder (wt%)	78	79	80	81
Binder (wt%)	22	21	20	19

removed from the ball-mill chamber in the inert atmosphere to prevent aluminum oxidization.

Then the mixed powders were weighted as the values listed in Table 2 and were blended with the melted binder using a mixer at the temperature of 85°C. The mixing temperature was between the decomposition and melting temperatures of the binder components.

The viscosity and rheological properties of the feedstocks were determined using a plate-plate measuring system by means of Physica MCR 301 Anton Paar Rheometer. The rheological behaviors of the feedstocks were studied at the temperature of 85°C and a shear rate range of 0.1–1000 s^{-1}. This instrument has capability of temperature adjusting, and therefore the temperature dependence of reological parameters could also be investigated. The Weir model is also applied to find the optimum feedstocks.

3 Results and discussion

3.1 Effect of powder loading on the rheological behavior of the feedstocks

Shear stress values versus shear rate of the prepared feedstocks are portrayed in Figure 2A. This figure shows that with increasing the shear rate, shear stress increases for all feedstocks. It can also be observed that the rates of increase associated with samples A and B are uniform, while some abrupt changes could be seen in the case of samples C and D in high shear rates. Since abrupt changes in shear stress are not desirable during injection molding, samples C and D are not suitable for injection.

The rheological behavior of feedstocks could be analyzed with the power law model to determine their type of flows:

$$\tau = k(\dot{\gamma})^n \quad (1)$$

where k is a constant, τ denotes the shear stress, $\dot{\gamma}$ is the shear rate, and n denotes the flow behavior index. The parameter of n is an indicator of shear sensitivity. If n<1, the behavior is pseudoplastic, and if n>1, the feedstock

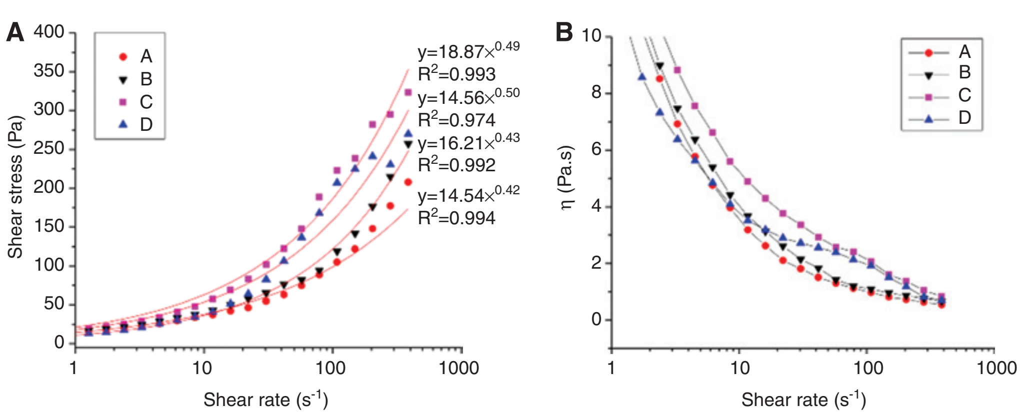

Figure 2 The rheological behavior of the feedstocks. (A) The adaptability of feedstocks with power law model, (B) viscosities of samples as a function of shear rates.

Table 3 Results of analyses of feedstocks with power law (the shear sensitivity values (n) as well as regression coefficients R^2).

Feedstock code	Power law model	
	R^2	Value n
A	0.994	0.41
B	0.992	0.43
C	0.993	0.49
D	0.974	0.50

behavior is dilatant. Also, Newtonian behavior is characterized by n=1. The analyses of the rheological behavior of all samples with the power law are summarized in Figure 2A and Table 3. It could be seen that all samples show pseudoplastic behavior, and the n value of sample A is the lowest. This indicates that sample A is the best sample for injection molding as the shear sensitivity of this sample is lowest.

The viscosities (η) of the feedstocks as a function of shear rates have also been depicted in Figure 2B. Typically, the viscosity of samples with higher powder loading should be higher than the others, while some deviation from this perception could be observed in Figure 2B. These deviations especially in low shear rates may be due to the lubricant nature of SiC particles as well as their texturing, which decreases the viscosity in feedstocks with high loading (sample D).

3.2 The homogeneity of the feedstocks

As mentioned earlier, one of the major concerns in injection molding process is the homogeneity of feedstock. One way of dealing with this is the observation of its torque value. In this regard, the homogeneity of feedstock can be predicted by observing the torque variation during mixing versus time. Uniform mixing was assumed to occur when the torque reached a steady state value [18]. The changes of torque value of feedstocks versus time are shown in Figure 3A. Results of this figure indicate that the stability of feedstock has been decreased by the increase of powder loading. It seems that we had the stability decrease after having the separation of the binder and powder. For further investigation, changes of the feedstock's viscosity with time are shown in Figure 3B. It can be seen that the viscosity first lowered and then went up in the case of sample C. The behavior could be related to the loss of structures which results in the reduction of viscosity in the first step. But as time passed, reformation of the structures occurred and the viscosity rose. In feedstock B, the viscosity increased with time until it reached a stable point. The phenomenon may be attributed to the formation of structures in the feedstock which could cause hard shearing in it. Since the stability of viscosity, even over short periods of time, is necessary for the mold to be filled, feedstock A is the desirable one for PIM due to its stable viscosity.

The SEM micrograph of feedstock A is illustrated in Figure 4. This image illustrates that the powder and binder were uniformly mixed in this feedstock without any bubble which verifies the results of the rheometry analyses.

3.3 Weir model

In order to select the most suitable powder loading in injection molding by rheometry results, the Weir model [19], which is proposed for polymers and semisolid materials, could be used. Equation (2) portrays the mathematical representation of this model.

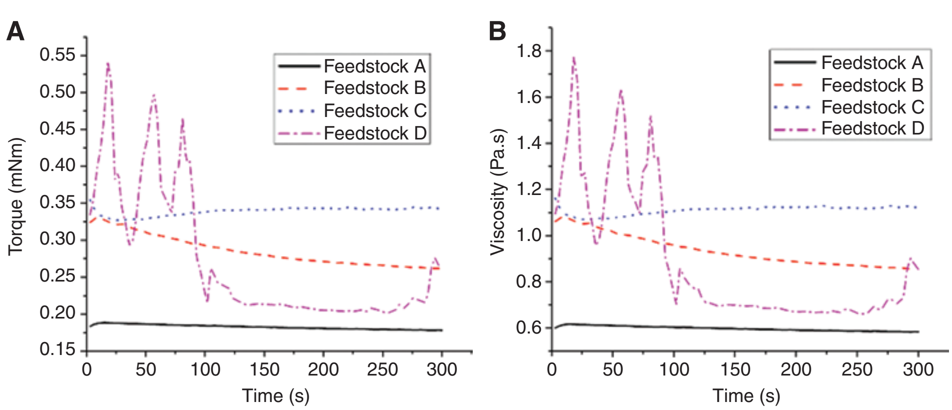

Figure 3 The estimation of feedstocks's homogeneity. (A) Variation of feedstock's torques and (B) variation of feedstock's viscosity, respectively.

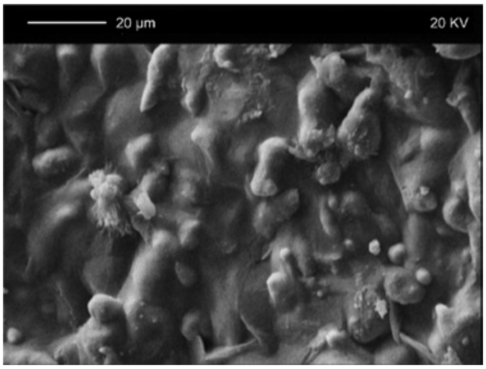

Figure 4 The scanning electron micrograph of feedstock denoted as A in Table 2.

$$\alpha = \frac{1}{\eta_0} \frac{\left|\partial \log \eta / \partial \log \dot{\gamma}\right|}{\partial \log \eta / \partial (1/T)} \quad (2)$$

In Equation (2), α is known as Weir model's constant and also moldability index, η denotes the viscosity, η_0 is referred to as a reference viscosity, and T and γ are temperature and shear rate, respectively. The higher value of moldability index (α) is pleasing since feedstocks with low η values are prone to the separation of powder and binder [16, 19, 20].

The moldability index for different feedstocks at the shear rate of 100(1/s) and the temperature of 85°C were calculated as a stability indicator of those, and the results are reported in Figure 5. Considering these figures, sample A has the highest moldability index, and therefore it would be chosen as the desired critical powder loading.

3.4 Calculation of flow activation energy

Viscosity of the feedstocks depends on temperature by Arrhenius' equation:

$$\eta = \eta_0 \exp(E/RT) \quad (3)$$

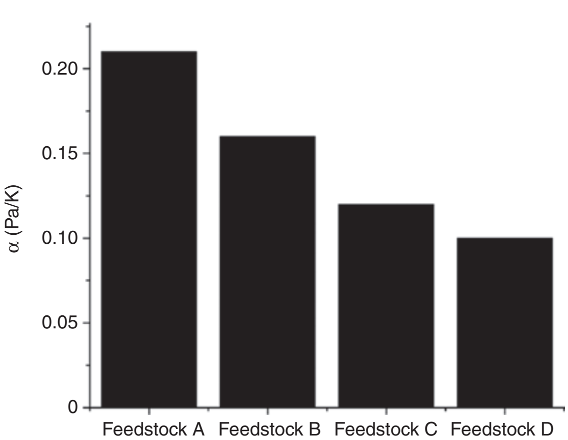

Figure 5 Evaluation of alpha values to determine the optimal powder loading.

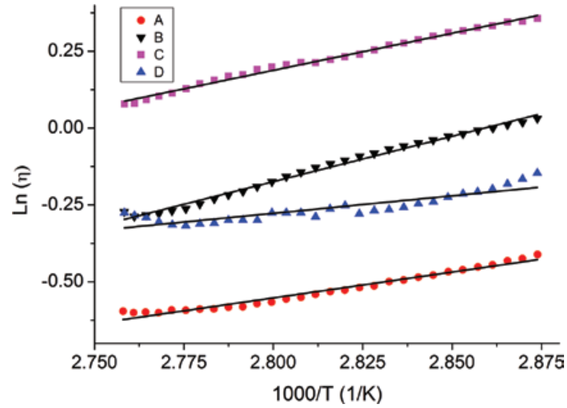

Figure 6 Plot of Ln(η) versus 1000/T for the prepared feedstocks.

where η_0 denotes viscosity at reference temperature, E is flow activation energy, R is the universal gas constant, and T denotes the temperature. The E value is indicator of the sensitivity of viscosity to temperature. If the value of E is low, the viscosity is less sensitive to temperature variations, and this results in fabrication of defect-free parts. The slopes of Ln (η) versus $1/T$ for all samples, as shown in Figure 6, are equal to the flow activation energy (E). The obtained results are also listed in Table 4. It can be seen that sample D has the lowest E value, but the regression coefficient of linear fit is low (<0.9), which indicates the high uncertainty of E value calculated for this sample. Omitting this sample, sample A has the lowest E value which indicates that the viscosity of this sample has less sensitivity to temperature. Therefore, it is suitable for injection molding in industrial process where the temperature control is not easy and high stability of viscosity is crucial.

4 Conclusion

The rheological behaviors of feedstocks containing 95 wt% aluminum and 5 wt% silicon carbide for preparation of Al/SiC nanocomposite with low-pressure injection molding method were investigated. Critical powder loading for these feedstocks was determined by studying

Table 4 The flow activation energies (E values) of feedstocks and regression coefficients of linear fit to their corresponding data.

Feedstock	E (kJ/mol)	Regression coefficient (R^2)
A	13.97	0.94
B	24.44	0.98
C	20.04	0.98
D	9.39	0.77

their homogeneity and rheological behavior as well as the application of Weir and power law models. The thermal flow activation energies of all samples have also been determined by studying the temperature dependence of viscosities of samples. The results showed that the feedstock containing 78 wt% of powder loading is the optimum one for preparation of Al/SiC nanocomposites by low-pressure injection molding. The SEM image also verifies this conclusion.

Acknowledgments: The authors thank Y. Ganjkhanlou for his assistance in the preparation of this paper.

Received September 4, 2013; accepted April 5, 2014; previously published online June 5, 2014

References

[1] Wang H, Zhang R, Hu X, Wang C-A, Huang Y. *J. Mater. Process. Technol*. 2008, 197, 43–48.
[2] Sahin Y. *Mater. Des*. 2003, 24, 671–679.
[3] Zhang XN, Geng L, Wang GS. *J. Mater. Process. Technol*. 2006, 176, 146–151.
[4] Zhaoa N, Nashb P, Yang X. *J. Mater. Process. Technol*. 2005, 170, 586–592.
[5] Mallik S, Ekere N, Best C, Bhatti R. *Appl. Therm. Eng*. 2010, 31, 355–362.
[6] Huang B, Liang S, Qu X. *J. Mater. Process. Technol*. 2003, 137, 132–137.
[7] Thomas-Vielma P, Cervera A, Levenfeld B, Varez A. *J. Eur. Ceram. Soc*. 2008, 28, 763–771.
[8] Loh NH, Tor SB, Khor KA. *J. Mater. Process. Technol*. 2001, 108, 398–407.
[9] Sotomayor ME, Várez A, Levenfeld B. *Powder Technol.* 2010, 200, 30–36.
[10] Yang W-W, Yang K-Y, Hon M-H. *Mater. Chem. Phys*. 2002, 78, 416–424.
[11] Li W-L. *Micro Nano Lett*. 2009, 4, 44–47.
[12] Namburu PK, Kulkarni DP, Dandekar A, Das DK. *Micro Nano Lett*. 2007, 2, 67–71.
[13] Thian ES, Loh NH, Khor KA, Tor SB. *Mater. Lett*. 2002, 56, 522–532.
[14] Suri P, Atre SV, German RM, Souza JPd. *Mater. Sci. Eng. A* 2003, 356, 337–344.
[15] Li Y, Li L, Khalil KA. *J. Mater. Process. Technol*. 2007, 183, 432–439.
[16] Agote I, Odriozola A, Gutierrez M, Santamarı A, Quintanilla J, Coupelle P, Soares J. *J. Eur. Ceram. Soc*. 2001, 21, 2843–2853.
[17] Hidalgo J, Jiménez-Morales A, Torralba JM. *J. Eur. Ceram. Soc*. 2012, 32, 4063–4072.
[18] Supati R, Loh NH, Khor KA, Tor SB. *Mater. Lett*. 2000, 46, 109–114.
[19] Weir FE, Doyle ME, Norton DG. *S.P.E. Trans*. 1963, 3, 32–336.
[20] Khakbiz M, Simchi A, Bagheri R. *Mater. Sci. Eng. A* 2005, 407, 105–113.